

UNCLASSIFIED

DEPARTMENT OF DEFENCE

AR-001-667

DEFENCE SCIENCE AND TECHNOLOGY ORGANISATION

ELECTRONICS RESEARCH LABORATORY

TECHNICAL REPORT

ERL-0077-TR

THE MEASUREMENT OF TEMPERATURE INSTABILITIES AND THEIR EFFECT  
ON THE LIQUID PHASE EPITAXIAL GROWTH OF GALLIUM ARSENIDE

M. Folkard

S U M M A R Y

Epitaxial layers grown on gallium arsenide substrates using the steady state temperature gradient form of liquid phase epitaxy have a much larger growth rate than that calculated for diffusion-limited conditions. In addition, and of major importance for device fabrication, there is a large variation in epilayer thickness over the surface of a single sample, and non-reproducibility from sample to sample.

The present report describes various measurements of the temperature and its local variation within the gallium melt solution, and attempts to relate the observed variations and instabilities to the epitaxial layers actually grown.

Approved for Public Release

---

POSTAL ADDRESS: Chief Superintendent, Electronics Research Laboratory,  
Box 2151, G.P.O., Adelaide, South Australia, 5001.

---

UNCLASSIFIED

## TABLE OF CONTENTS

	Page No.
1. INTRODUCTION	1
2. THE CALCULATION OF GROWTH RATES	1 - 3
2.1 Slope of the liquidus curve	2
2.2 Diffusion coefficient	2
2.3 Solution temperature gradient	2
2.4 Predicted growth rates	2 - 3
3. OBSERVED GROWTH RATES	3 - 4
3.1 The growth vessel	3
3.2 Measurement of the epilayer heights	3
3.3 Observed epilayer heights	3
3.4 Discussion	4
4. TEMPERATURE PROFILE IN THE MELT	5 - 9
4.1 Single thermocouple probe	5
4.2 Differential thermocouple probe	6 - 9
4.3 Furnace temperature uniformity	9
5. CONCLUSIONS	9 - 10
6. ACKNOWLEDGEMENTS	10
REFERENCES	11

## LIST OF TABLES

1. DETERMINATION OF THE SOLUTION TEMPERATURE GRADIENT USING THE SINGLE THERMOCOUPLE PROBE	12
2. SERIES 'A' MEASUREMENTS WITH DIFFERENTIAL THERMOCOUPLE PROBE (Nominal temperature 800°C)	12
3. SERIES 'B' MEASUREMENTS WITH DIFFERENTIAL THERMOCOUPLE PROBE (Nominal temperature 800°C)	13
4. SERIES 'C' MEASUREMENTS WITH DIFFERENTIAL THERMOCOUPLE PROBE (Nominal temperature 800°C)	13
5. SERIES 'C' MEASUREMENTS WITH DIFFERENTIAL THERMOCOUPLE PROBE (Nominal temperature 700°C)	14
6. MEASUREMENTS IN HYDROGEN WITH DIFFERENTIAL THERMOCOUPLE PROBE (Nominal temperature 800°C)	14

## LIST OF FIGURES

1. Schematic diagram of the growth vessel used for epitaxial layer growth by the Steady State method
2. Schematic representation of spot heights for epitaxial layers grown at "average" temperatures of 800°C and 700°C. The left hand side of each diagram represents the edge of the substrate which was closest to the graphite peg used to hold the source block in position in the bottom of the growth vessel
3. Example of non-uniform epitaxial growth and simultaneous etching of the substrate surface, caused by large horizontal temperature gradients in the melt solution.  
(Sample 17, nominally 700°C for 4 hours)
4. Schematic of the temperature measuring system used with the single thermocouple probe
5. Typical example of the variation in results when the single thermocouple probe is lowered into or raised up out of the melt (40 divisions on the recorder = 100  $\mu$ V from probe = 2.4°C)
  - . lowering probe 0.82°C/cm
  - x raising probe 1.05°C/cm
6. (a) Schematic of the differential thermocouple probe assembly.  
(b) Enlarged view of the differential probe. The vertical distance between the two chromel-alumel junctions is 2.0 mm
7. Technique used to increase the measurement accuracy of the differential thermocouple probe
8. The linear relationship between the temperature gradient in the melt  $\left(\frac{\Delta T_s}{\Delta x}\right)$  and the applied furnace differential  $\Delta T$ .  
For a range of temperature differentials of -50°C to +50°C, the average slope  $\left(\frac{\Delta T_s}{\Delta x}\right) / \Delta T$  is  $3.85 \times 10^{-2}/\text{cm}$
9. Magnitude of the baseline "zero" drift on one occasion, when both top and bottom furnace temperature controllers were set on 33 mV (793°C) (average drift over the linear region shown is 10.6  $\mu$ V/hour)
10. Recorder trace from the differential thermocouple probe at an "average" temperature of 800°C. The furnace settings used to determine the baseline were  $T_{\text{top}} = T_{\text{bottom}} = 33 \text{ mV (793°C)}$  while those used for a nominal differential  $\Delta T$  of 50°C were  $T_{\text{top}} = 32 \text{ mV (769°C)}$  and  $T_{\text{bottom}} = 34 \text{ mV (818°C)}$ . The trace also demonstrates a typical baseline "zero" drift, in this example the drift is of magnitude  $\sim 2.3 \mu\text{V/hour}$
11. Temperature "overshoots" produced in the furnace by alteration of the top or bottom furnace temperature controllers

12. Axial variation of temperature along the furnace sections when both controllers are set to 33 mV (corresponding to 793°C)
  - + top element
  - . bottom element

## 1. INTRODUCTION

Cooling a gallium melt which is saturated with arsenic will result in the epitaxial deposition of a monocrystalline layer onto a single crystal gallium arsenide substrate placed in contact with the melt. This occurs, in part, because the solubility of a dilute constituent in a liquid solvent decreases with decreasing temperature. A variation of this method, which allows epitaxial growth to take place at a constant temperature, uses a temperature differential imposed across the melt solution by a split furnace whose upper element is maintained at a lower temperature than the bottom element. This temperature gradient across the melt provides a driving force for the diffusion of arsenic, dissolved from a gallium arsenide source, through the melt to the cooler substrate where it is deposited as an epitaxial layer of gallium arsenide.

The growth rates predicted under specified conditions using a diffusion model are much smaller than the rate of epilayer growth which is experimentally observed(ref.1). In addition, and of major importance for device fabrication, there is a large variation in epilayer thickness over the surface of a single sample, and non-reproducibility from sample to sample.

The present report describes various measurements of the temperature and its local variation within the melt solution, and attempts to relate the observed variation in epitaxial layer heights to these temperature variations.

## 2. THE CALCULATION OF GROWTH RATES

A mathematical formulation for the growth of epitaxial layers by the steady state method may be derived by assuming that diffusion of gallium arsenide through the melt is the rate-limiting process.

Such a treatment(ref.1) predicts a growth rate:

$$\frac{dh}{dt} = D \frac{\rho_{Ga}}{\rho_{GaAs}} \frac{M_{GaAs}}{M_{Ga}} \left( \frac{\Delta T_s}{\Delta x} \right) \left( \frac{dX_{As}^1}{dT} \right)_{T_{sub}}$$

where

$$\left( \frac{dX_{As}^1}{dT} \right)_{T_{sub}} = \frac{d}{dT} \left[ \frac{X_{As}(T_{source})}{1 - 2X_{As}(T_{source})} - \frac{X_{As}(T_{sub})}{1 - 2X_{As}(T_{sub})} \right]$$

Here,  $X_{As}(T)$  = solubility of As in Ga at temperature T

D = diffusion coefficient of As in Ga

$\rho_{Ga}$  = density of liquid gallium (5.95 g/cc)

$\rho_{GaAs}$  = density of gallium arsenide (5.32 g/cc)

$M_{Ga}$  = atomic weight of gallium (69.7)

$M_{GaAs}$  = molecular weight of gallium arsenide (144.6)

$\left( \frac{\Delta T_s}{\Delta x} \right)$  = temperature gradient within the melt solution

$T_{source}$  = temperature of the source material

$T_{sub}$  = temperature of the substrate surface.

To estimate the rate of epilayer growth it is necessary to obtain relevant values for the slope of the liquidus curve, the diffusion coefficient, and the solution temperature gradient.

## 2.1 Slope of the liquidus curve

The slope  $\frac{dX_{As}^1}{dT}(T)$  of the liquidus curve is obtained from the solubility data of Hall(ref.2) which receives independent verification from Hsieh(ref.3) in the limited temperature region near 800°C. A smooth curve drawn through Hall's experimental data, with almost every experimental data point lying actually on the smooth curve, yields the values

$$T = 700^{\circ}\text{C}, \text{ liquidus slope} = 0.90 \times 10^{-4}/^{\circ}\text{C}$$

$$T = 800^{\circ}\text{C}, \text{ liquidus slope} = 2.78 \times 10^{-4}/^{\circ}\text{C}$$

(These values are considered accurate to within a few percent.)

## 2.2 Diffusion coefficient D

There have been no direct measurements of the diffusion of As or GaAs in gallium solution. Estimates for D have been made by comparing experimental growth rates with the predictions of various mathematical theories based on diffusion-limited growth, and obtaining "best fit" values for D. There is a large spread in the values so obtained, for example from  $1 \times 10^{-5}$  to  $10 \times 10^{-5} \text{ cm}^2/\text{s}$  at 800°C, with some investigators claiming no temperature dependence and others claiming an exponential dependence (ref.3 to 7). The values

$$T = 700^{\circ}\text{C} \quad D = 3 \times 10^{-5} \text{ cm}^2/\text{s}$$

$$T = 800^{\circ}\text{C} \quad D = 5 \times 10^{-5} \text{ cm}^2/\text{s}$$

are consistent with the general trend of the majority of these references, and so have been used in the present case.

## 2.3 Solution temperature gradient $\frac{\Delta T_s}{\Delta x}$

To determine the temperature gradient within the melt, a pyrolytic graphite probe was constructed containing a chromel-alumel thermocouple. Full details of the probe and the methods of measurement are given in Section 4. The repeatability of these measurements was poor, as can be seen in Tables 1 to 3, but they did indicate that the solution temperature gradient was relatively independent of the actual furnace temperatures for a given differential  $\Delta T$  between top and bottom furnace elements. For an external differential of 50°C, the solution temperature gradient was found to be approximately 4.2°C/cm at 700°C (Table 4) and 4.6°C/cm at 800°C (Tables 1 to 3).

## 2.4 Predicted growth rates

Using the values shown below, the predicted growth rates become

$$1.0 \text{ } \mu/\text{hour at } 700^{\circ}\text{C, and}$$

$$5.3 \text{ } \mu/\text{hour at } 800^{\circ}\text{C.}$$

$T(^{\circ}\text{C})$	$D \text{ (cm}^2/\text{s)}$	$\left( \text{slope } X_{\text{As}}^1 (T) - T \right)_{T_{\text{sub}}}$	$\left( \frac{\Delta T_s}{\Delta x} \right) ^{\circ}\text{C/cm}$
700	$3 \times 10^{-5}$	$0.90 \times 10^{-4}$	4.2
800	$5 \times 10^{-5}$	$2.78 \times 10^{-4}$	4.6

### 3. OBSERVED GROWTH RATES

The following results apply for a steady state temperature differential  $\Delta T$  of  $50^{\circ}\text{C}$ , and indicate the order of magnitude of the growth rates obtained for 2 hours at  $800^{\circ}\text{C}$  or 4 hours at  $700^{\circ}\text{C}$ . Before presenting the observed growth rates, some details on the apparatus and measuring technique are relevant.

#### 3.1 The growth vessel

The growth vessel of vitreous carbon is shown in figure 1, where it can be seen that the source block is held down by a graphite peg of length 31 mm and square cross section of side 6 mm. The substrate (5 mm x 10 mm) is held by suction onto a pyrolytic graphite holder of length 36 mm and area 13 mm x 7 mm at substrate and 19 mm x 9 mm at top. Movement of the substrate and holder is manually controlled from outside the furnace by a long quartz rod, and growth is initiated (and terminated) by rotating the substrate holder down into (or up out of) the melt solution.

#### 3.2 Measurement of the epilayer heights

Spot heights of the grown layers were found by breaking each sample into sections along (110) planes (shown in figure 2 by faint lines) then staining for 15 to 40 s with a solution of  $\text{HF} : \text{HNO}_3 : \text{H}_2\text{O} = 1:3:4$ . Differences in electron affinities in the differently doped regions affect the rate at which GaAs reacts with the staining solution, and the difference in etching rates causes the junction to become visible. A Zeiss KK08 reflected light microscope was used with a Nomarski differential interference contrast attachment and a magnification of 128X. Calibration of the eyepiece scale yielded a value of  $6.8 \mu$  per smallest division at this magnification, so that the resolution of the tabulated layer thickness is within a few microns in each case.

#### 3.3 Observed epilayer heights

Figure 2 is a schematic representation of the epilayer thickness for eight individual samples. The left hand side of each diagram represents the edge of the substrate which was closest to the graphite peg used to hold the solute block in position in the bottom of the crucible. Although the results from each sample were different the general trend shows a thicker grown layer on the side of the substrate nearer the graphite peg. This suggests that the portion of the melt near the graphite peg may be cooler than elsewhere. The variable epilayer heights over a single sample, and the non-repeatability from sample to sample quite strongly suggest that processes other than simple diffusion of gallium arsenide through the melt are taking place. It is also evident from figure 2 that the observed growth rates are greatly in excess of the values calculated in Section 2. A very rough estimate for the "average" growth rate for the samples shown in figure 2 would be  $5 \mu/\text{hour}$  and  $15 \mu/\text{hour}$ , at  $700^{\circ}\text{C}$  and  $800^{\circ}\text{C}$ , compared to the calculated values of  $1 \mu/\text{hour}$  and  $5 \mu/\text{hour}$  respectively. However, the dominant feature is the non-uniformity of the growth.

### 3.4 Discussion

Uniform growth rates much greater than those predicted from the diffusion model, and more in accord with the "average" magnitudes observed, might be explained by considering either

(a) a temperature gradient  $\frac{\Delta T}{\Delta x}$  of about  $15^{\circ}\text{C}/\text{cm}$  within the solution,

or (b) a much greater value for  $D$  than that used in the calculations of Section 2.

Possibility (a) is improbable because the total temperature differential of  $50^{\circ}\text{C}$  occurs over a distance in excess of 6 cm, and measurements later described in the present report (Table 5) indicate the temperature gradient in the hydrogen atmosphere to be  $8.0^{\circ}\text{C}/\text{cm}$ . Possibility (b) is also unable to account for the increased growth rate. Even considering the largest value of  $10 \times 10^{-5} \text{ cm}^2/\text{s}$  estimated for  $D$  from the wide range of values in references 3 to 7, the predicted growth rate using the diffusion model is still only  $\sim 10.6 \mu/\text{hour}$ .

However, the dominant feature observed from the various samples in figure 2 is the non-uniformity of grown layer heights over the area of each sample, which can in no way be accounted for by the simple diffusion model. A plausible explanation for the observed situation is that kinetic processes such as convection might be occurring within the melt in addition to the diffusion of arsenic through the melt. To test this hypothesis, some variation to the standard experimental procedures of Runs 1 to 15 were made. In these earlier experiments, the epitaxial layers had been grown from melts containing 30 g of gallium, which filled the crucible to 7 mm above the solute block, while the maximum height of the substrate above the solute block was 5 mm. In Runs 16 to 20, the melt was increased to 60 g of gallium, which brings the liquid surface about 13 mm above the solute block, so that the liquid surface is now at least 8 mm above the growth plane. Consequently there is a large volume of melt above the substrate and we might expect convective effects to be increased by this larger melt volume. In these circumstances the effect on a substrate at  $700^{\circ}\text{C}$  for 4 hours was to grow a layer on the side of the substrate near the graphite peg and to etch material away from the side further into the melt (see figure 3). A similar result was obtained at  $800^{\circ}\text{C}$  for 2 hours, while at the higher temperature a "growth" time of 4 hours resulted in the substrate being etched all over, though to a lesser extent near the peg than remote from it. The substrate - nominally at a cooler temperature than the solute block - had been partially dissolved although there was a large excess of solute present. In addition, the solute block exhibited a definite pattern of channels on its surface. Far from the graphite peg, the solute block had been completely dissolved while no dissolution of material whatever had taken place actually under the peg. This provides definite evidence for non-uniformities within the growth environment, and makes it imperative to study the growth kinetics more closely. The first step in determining how convection and associated processes may be developing is to determine the variation in temperature and temperature gradient throughout the actual melt. This involves precise temperature profiling under specified conditions.

#### 4. TEMPERATURE PROFILE IN THE MELT

Preliminary measurements using a single thermocouple probe are first described, followed by the more detailed measurements in which a differential thermocouple probe was used. In each case the monitoring system simulated the experimental situation as closely as possible, aiming to determine the temperature conditions during an actual growth run rather than the conditions in an unperturbed melt. Since the thermal conductivity of the pyrolytic graphite substrate holder itself must alter the temperature gradient within the solution (the electrical and thermal properties of pyrolytic graphite are markedly anisotropic) the probe was made of the same dimensions as the substrate holder, and the same quartz dipping rod arrangement was used.

##### 4.1 Single Thermocouple Probe

The initial temperature measurements were taken with a chromel-alumel thermocouple of 0.025 inches diameter wire. Quartz capillary tubes were placed over each of the leads to prevent contact with each other and the graphite probe. The "hot" junction of the thermocouple was encased in quartz which was ground flat and held against the bottom of the graphite probe by a small pyrolytic graphite screw, in the region where the substrate would normally be positioned. Although this screw prevented the thermocouple from reaching closer than 2 mm to the crucible base, it was felt a not-too-unreasonable perturbation for a first attempt, since actual growths are carried out at distances greater than 2 mm above the crucible bottom.

The probe was dipped into a Ga melt of depth about 18 mm and raised or lowered to simulate the geometry used for epitaxial growth. The melt temperature  $T_s(x)$  was monitored as a function of distance  $x$  above the bottom of the crucible using a Rikadenki B-24 recorder which was calibrated with a Cambridge Model 44228 potentiometer bridge. Comparison of  $T_s(x)$  at different positions within the melt allowed a temperature profile to be obtained.

To increase the accuracy of measurement, an off-set voltage arrangement using the Cambridge potentiometer was set up as shown in figure 4. It was possible by this means to make differential temperature measurement with great accuracy because only short term stability of the thermocouple and that of the off-set voltage are of first order significance in determining the accuracy of the difference between any two of the readings.

Although each individual set of measurements was reasonably self-consistent, the repeatability of measurements from day to day, or even in successive raisings and lowerings of the probe, was poor. The readings from a typical experiment are shown in figure 5, while Table 1 demonstrates the variation in results observed from day to day. For the conditions under which most of the epitaxial growths were carried out ( $T_{\text{top}} = 769^\circ\text{C}$ ,  $T_{\text{bottom}} = 818^\circ\text{C}$ ,  $\Delta T$  nominally  $50^\circ\text{C}$ ) the temperature gradient using this probe was found to be of the order of  $1^\circ\text{C}/\text{cm}$ .

In these experiments, no correction was applied to the results to allow for the change in relative depth of solution with displacement by the measuring probe (in any case corrections would be of minor significance here where a large volume of Ga was used, although it might be more significant in the situation where only a small volume of melt was used). Of more importance however, is the assumption that the temperature profile is not modified by moving the probe.

## 4.2 Differential Thermocouple Probe

To overcome some of the limitations of the single thermocouple measurements, a differential thermocouple was constructed and used with the same graphite probe and dipping rod arrangement as has already been described.

This time the wires were of 0.005" diameter, which caused some difficulties as they became brittle after sustained operation at high temperature in the reducing atmosphere and sometimes broke. When this occurred, the furnace had to be cooled and the entire apparatus dismantled, the wires repaired and the apparatus reassembled, causing considerable delay. The vertical separation of the two "hot" junctions was 2.0 mm, formed by a length of chromel wire, with the leadout wires made from alumel. Again the thermocouple was encased in thin quartz to prevent melting by the hot gallium solution, and the leadout wires were threaded with quartz capillary to prevent contact and possible shorting with each other and with the graphite probe. A schematic diagram of the probe assembly is shown in figure 6.

To increase the accuracy of measurements, the arrangement shown in figure 7 was used. The Hewlett-Packard 419A DC null voltmeter output terminal was adjusted to read  $(1.0000 \pm 0.0005)$  volts for full-scale deflection on any input range of the digital voltmeter. At the same time the zero and gain of the Rikadenki recorder were adjusted on the 1 volt input scale. Once set up, these instruments were found to remain exceptionally stable over several weeks operation. By using the 100  $\mu$ V range on the HP voltmeter, the 25 cm scale on the Rikadenki recorder then corresponds to only  $2.4^\circ\text{C}$ , so that this arrangement allowed the detection of very small temperature differences.

Initially the probe was positioned near, but not actually touching, the bottom of the crucible in a melt of 30 gm Ga. This melt fills the crucible (with graphite peg present) to a height of 7 mm, which corresponds to the conditions of Runs 1 to 15 earlier described. With the probe in this position the temperature differential  $\Delta T_P$  across the differential thermocouple was monitored as the furnace differential  $\Delta T$  was altered, keeping the "average" furnace temperature at  $793^\circ\text{C}$  (33 mV on the chromel-alumel

monitoring thermocouple). Using the equation  $\frac{\Delta T_s}{\Delta x} = \frac{\Delta T_P}{0.2} ^\circ\text{C/cm}$ , the

relationship (see figure 8) between  $\left(\frac{\Delta T_s}{\Delta x}\right)$  and  $\Delta T$  was found to be

$$\left(\frac{\Delta T_s}{\Delta x}\right) = 3.85 \times 10^{-2} \frac{^\circ\text{C/cm}}{^\circ\text{C}} \cdot \frac{\Delta T}{\Delta T}$$

It should be observed from figure 8 that although linearity is shown, direct proportionality of  $\left(\frac{\Delta T_s}{\Delta x}\right)$  and  $\Delta T$  does not occur. A simple treatment by McRae(ref.8) which considers that heat transfer from the furnace to the melt takes place only by radiation, predicts that

$$\left(\frac{\Delta T_s}{\Delta x}\right) = \gamma T^4 \cdot \Delta T + \text{terms in } (\Delta T)^2$$

Note that as  $\Delta T$  goes to zero, this equation predicts that  $\left(\frac{\Delta T_s}{\Delta x}\right)$  will also vanish. Figure 8 shows that experiment does not support this prediction

and we are forced to conclude that  $\left(\frac{\Delta T_s}{\Delta x}\right)$  and  $\Delta T$  are not directly proportional.

Moreover, it soon became apparent from these measurements, the value of  $\left(\frac{\Delta T_s}{\Delta x}\right)$  when  $\Delta T = 0$  is far from constant, even when the probe is not moved at all. In fact when the probe differential temperature  $\Delta T_p$  was monitored over extended periods with  $\Delta T = 0$ , a linear "drift" with time was found, of the order of several microvolts/hour. Furthermore when similar measurements are carried out under sensibly constant conditions (probe position unaltered) over periods of several days, the observed drift may be positive or negative. Figure 9 shows the magnitude of the baseline drift on one occasion over a 12 hour period when both furnace controls were set to 33 mV (793°C). From Table 2, where measurements were made over a 5 day period, it can be seen that the baseline drift varies in an irregular manner, which makes one suspect that it might be an instrumentally induced effect.

For the Series A measurements recorded in Table 2, the temperature controller of the bottom furnace element was initially set at 34 mV (818°C) while the top controller was set to 32 mV (769°C), producing a nominal temperature difference  $\Delta T$  of 50°C. (These conditions, when used for epitaxial layer growths, are referred to in the present report as "growth at 800°C".) The voltage reading  $(T_p)_1$ , from the differential probe was recorded under these conditions, after which both top and bottom furnace controllers were reset to 33 mV (corresponding to 793°C). When the furnace had stabilised at these new conditions with  $\Delta T = 0$  another probe voltage reading  $(T_p)_2$  was recorded.

The voltage from the probe was monitored continuously on a recorder, as shown for a typical experiment in figure 10. The slope of the trace under constant applied conditions allowed an estimation of the baseline drift during the time between the measurement of  $(T_p)_1$  and  $(T_p)_2$ , whilst the difference between  $(T_p)_1$  and  $(T_p)_2$  was considered as the real measure of

$\Delta T_p$  induced by the external furnace differential of  $\Delta T = 50^\circ\text{C}$ . (The voltage overshoot which is observed from the probe whenever the furnace controllers are altered can be directly explained by the furnace temperature overshoots which are clearly demonstrated in figure 11.) The value of  $\Delta T_p$  so obtained and corrected for baseline drift was then converted to an equivalent temperature gradient in  $^\circ\text{C}/\text{cm}$ . It is of interest to note that the measured temperature gradient increased from a value of about  $2.0^\circ\text{C}/\text{cm}$  during the early period of operation at 800°C, to approximately  $(4.6 \pm 0.4)^\circ\text{C}/\text{cm}$  after an extended period. Additional measurements showed, as expected from the form of the grown layers described in previous sections, that the temperature gradient decreased with distance away from the graphite peg.

Another set of measurements, referred to as Series B and shown in Table 3 were carried out after the thermocouple had broken and been repaired. Although the "relative" temperature gradient for the first day's operation in Series B, did not differ appreciably from the first day's operation in Series A, and the magnitudes of the baseline drift were similar, the "absolute" probe readings were very much greater in the Series B measurements. The probe was then dismantled, both alumel leadout wires were sheathed in quartz capillary and threaded down a cylindrical copper shielding cable, which was in turn threaded through the hollow quartz dipping rod. By using this careful shielding it was hoped to

- (i) reduce the noise on the output signal of the differential thermocouple

- (ii) reduce or eliminate the variable baseline drift on the output signal which occurred under supposedly steady furnace conditions
- (iii) reduce or even eliminate whatever effects were causing the variable (and sometimes very large) readings  $(T_p)_2$  on the differential

thermocouple probe when  $\Delta T = 0$ , i.e. when no temperature differential is applied across the furnace.

Although the shielding reduced the noise level a great deal, and also eliminated the baseline drift once the probe had been in the melt for several days (Tables 4 to 6), the results of Series C measurements did not allow any quantitative conclusions to be made regarding the effects causing a non-zero probe reading  $(T_p)_2$  for  $\Delta T = 0$ .

All the measurements in Tables 2 to 4 were made at a nominal "average" temperature of  $800^\circ\text{C}$ , with either the top furnace controller set to 34 mV ( $818^\circ\text{C}$ ) and the bottom set to 32 mV ( $769^\circ\text{C}$ ), or the top and bottom set together to 33 mV ( $793^\circ\text{C}$ ). Further measurements made during Series C with bottom and top furnace settings of 30 mV ( $721^\circ\text{C}$ ) and 28 mV ( $673^\circ\text{C}$ ) respectively or both elements at 29 mV ( $697^\circ\text{C}$ ) are presented in Table 5. These readings at a nominal "average" temperature of  $700^\circ\text{C}$  produced a value for the solution temperature gradient  $\frac{\Delta T_s}{\Delta x}$  of approximately  $4.2^\circ\text{C/cm}$ . The results of  $4.6^\circ\text{C/cm}$  at an average temperature of  $800^\circ\text{C}$  and  $4.2^\circ\text{C/cm}$  at an average temperature of  $700^\circ\text{C}$ , show that  $\left(\frac{\Delta T_s}{\Delta x}\right)$  varies only slowly with the average furnace temperature provided that  $\Delta T$  is kept constant.

The temperature gradient in the flowing hydrogen stream above the crucible was measured by raising the probe vertically out of the melt as far as it would go towards the top of the quartz furnace tube. It was visibly checked that no Ga remained on the probe before a series of measurements were made at an average furnace temperature of  $800^\circ\text{C}$  and a differential of  $50^\circ\text{C}$ , in similar fashion to those made when the probe is in the melt. The observed value

$\frac{\Delta T_H}{\Delta x}_2$  of  $8.0^\circ\text{C/cm}$  shown in Table 6, agrees well with the known applied  $\Delta T$  of  $50^\circ\text{C}$  applied over a 6 cm region, and so provides confidence in the results derived using this probe.

However, on reviewing all the information shown in Tables 2 to 4, it is evident that in each case the early measurements yield a value for the solution temperature gradient of about  $2^\circ\text{C/cm}$ , while those measurements taken after the furnace had been on for an extended period (several days) all yield values close to  $4.6^\circ\text{C/cm}$ . Insufficient time remained to investigate this phenomenon, but it possibly is consistent with the observation that about 24 hours "equilibration" time between the melt and the source material is necessary before good epitaxial layers can be grown routinely (ref.1).

The conclusions drawn from these temperature probing experiments using the differential thermocouple probe are as follows:

"Average" Temperature $T(^{\circ}\text{C})$	Furnace temperature differential $\Delta T (^{\circ}\text{C})$	Solution temperature Gradient $\frac{\Delta T_s}{\Delta x} (^{\circ}\text{C/cm})$	Temperature gradient in Hydrogen atmosphere $\left(\frac{\Delta T_H}{\Delta x}\right)_2 (^{\circ}\text{C/cm})$
$700^\circ\text{C}$	$50^\circ\text{C}$	4.2	$8.0^\circ\text{C/cm}$
$800^\circ\text{C}$	$50^\circ\text{C}$	4.6	

It must also be remembered that  $\left(\frac{\Delta T_s}{\Delta x}\right)$  varies within the actual solution, tending to decrease near the graphite peg, and also to decrease towards the bottom of the crucible - so that the values tabulated above are not of high absolute accuracy.

#### 4.3 Furnace temperature uniformity

Because of the substantial variation in the value for  $\left(\frac{\Delta T_s}{\Delta x}\right)$  obtained from day to day with the single thermocouple probe, some measurements of the axial variation of furnace temperature itself were carried out. Top and bottom sections of the Marshal split furnace can be controlled independently, and each section consists of 3 appropriately connected elements. Temperature control in each section is maintained by feedback from a chromel-alumel thermocouple fixed near the mid-position of each centre element.

The temperature variations along both top and bottom sections of the furnace were determined by moving independent chromel-alumel monitoring thermocouples axially along each section, and measuring the output voltage with the Cambridge potentiometer. As shown in figure 12, even when both controllers are set to the same temperature of 793°C (33 mV), the axial variation is significant, with a steady increase in temperature out to a distance of about 12 cm from the centre, followed by a rapid decrease as the open ends of the furnace exert increasing influence. Although the bottom element exhibits a fairly constant temperature near the centre, the top element varies by about 25°C over the region within 4 cm of the centre. Thus the actual temperature differential within the furnace will differ from the applied value (Nominally 50°C during the epilayer growth runs reported in reference 1, and for the temperature probing measurements described in this report) by up to 25°C over a distance of just a few cm.

Since the furnace differential is not constant even over the central region, then small differences from run-to-run in positioning the crucible and substrate holder (or probe) will result in a different temperature gradient within the growth solution. In addition, differences in temperature gradient will occur over the substrate area, with the side furthest from the furnace being at a higher temperature (or, alternatively, thought of as under the influence of a reduced solution temperature gradient) than the side near the centre of the furnace. It will be recalled from Section 3 that the grown layers were in general thickest on the side near the centre of the furnace (i.e. near the graphite peg), and that when etching occurred in Runs 16 to 20, the etching was greater on the side away from the graphite peg. These experimental observations are consistent with the observed reduction in temperature gradient and increase in average furnace temperature with increasing distance from the centre of the furnace elements.

#### 5. CONCLUSIONS

The vertical temperature gradients  $\left(\frac{\Delta T_s}{\Delta x}\right)$  which were measured within the gallium melt do not account for the observed thicknesses of the grown epitaxial layers if diffusive transfer of gallium arsenide through the gallium melt is considered as the only process contributing to the epitaxial growth. The variability in thickness of these layers, not only from sample to sample but in fact over the area of each individual sample, quite strongly suggests that additional processes are occurring within the melt.

A plausible explanation for the observed situation is that kinetic processes such as convection might be taking place. The axial variations within the melt, which were found in Section 4, may set up instabilities which result in cellular convection. Because there are both horizontal and vertical temperature variations within the melt, and the solubility of arsenic in gallium is temperature dependent, the solute concentration will vary horizontally as well as vertically. The transfer of solute material to the growth interface will be increased by this natural convection, thus increasing the growth rate. The fluid motion may create unstable conditions at the interface, with any point on the surface of the growing layer being subject to a supersaturation which varies with time. Such variations could explain the variable thickness of the epilayer across a given sample, and also the irregular surface morphology which is observed.

## 6. ACKNOWLEDGEMENTS

I am indebted to the Electrical Engineering Department of the University of Adelaide for providing laboratory facilities, and to Mr G. Pook and Mr G. Allison for their sustained technical assistance. I would also like to thank Dr R. Hartley for his critical appraisal of this manuscript.

## REFERENCES

- | No. | Author                          | Title   |
|-----|---------------------------------|---|
| 1   | Folkard, M.A.                   | "Liquid Phase Epitaxial Growth of Gallium Arsenide".<br>DRCS Technical Report ERL-0078-TR   |
| 2   | Hall, R.N.                      | "Solubility of III-V Compound Semiconductors in Column III Liquids".<br>J. Electrochem. Soc. Vol. 110, p385-388,<br>May 1963  |
| 3   | Hsieh, J.J.                     | "Thickness and Surface Morphology of GaAs LPE Layers Grown by Supercooling, Step-cooling, Equilibrium Cooling, and Two-phase Solution Techniques".<br>J. Crystal Growth Vol. 27, p49-61,<br>December 1974 |
| 4   | Rode, D.L.                      | "Isothermal Diffusion Theory of L.P.E.: GaAs, GaP, Bubble Garnet".<br>J. Crystal Growth Vol. 20, p13-23,<br>August 1973   |
| 5   | Moon, R.L. and Kinoshita, J.    | "Comparison of Theory and Experiment for LPE Layer Thickness of GaAs and GaAs Alloys".<br>J. Crystal Growth Vol. 21, p149-154,<br>January 1974  |
| 6   | Dawson, L.R.                    | "Near-Equilibrium LPE Growth of GaAs-Ga <sub>1-x</sub> Al <sub>x</sub> As Double Heterostructures".<br>J. Crystal Growth Vol. 27, p86-96,<br>December 1974  |
| 7   | Mlavsky, A.I. and Weinstein, M. | "Crystal Growth of GaAs from Ga by a Travelling Solvent Method".<br>J. Appl. Phys. Vol. 34, No. 9, p2885-2892,<br>September 1963  |
| 8   | McRae, C.J. and Griffin, D.W.   | "Liquid Phase Epitaxy of GaAs-Growth Control".<br>Proc. NELCON '74, University of Auckland,<br>26 to 30 August 1974   |

TABLE 1. DETERMINATION OF THE SOLUTION TEMPERATURE GRADIENT USING THE SINGLE THERMOCOUPLE PROBE

Day	Technique	Solution ( $^{\circ}\text{C}/\text{cm}$ ) temperature gradient
1	lowering probe	1.19
2	lowering probe	0.77
3	lowering probe raising probe	0.53 0.74
4	lowering probe raising probe	0.82 1.05

TABLE 2. SERIES 'A' MEASUREMENTS WITH DIFFERENTIAL THERMOCOUPLE PROBE (NOMINAL TEMPERATURE  $800^{\circ}\text{C}$ )

	Furnace settings (mV)	Absolute readings probe ( $\mu\text{V}$ )		Relative readings probe ( $\mu\text{V}$ )		Baseline drift ( $\mu\text{V}/\text{hour}$ )
		$(T_p)_1$	$(T_p)_2$	$\Delta T_p$	$\left(\frac{\Delta T_s}{\Delta x}\right)^{\circ}\text{C}/\text{cm}$	
4/7/75	32-34 33-33	58.9	48.1	17.1	2.05	+2.5
5/7/75	32-34 33-33 32-34 33-33	44.3 39.2	8.9 3.8	35.4 35.4	4.25 4.25	-1.3
6/7/75	32-34 33-33 33-33 32-34	47.7 64.8	10.4 25.0	37.3 39.8	4.48 4.78	+2.6
7/7/75	32-34 33-33 33-33 32-34	102.5 112.5	64.3 70.0	38.2 42.5	4.58 5.10	+2.0
8/7/75	32-34 33-33 32-34	110.1 117.6	73.2	36.9 44.4	4.29 5.15	+5.0

32 mV setting corresponds to  $769^{\circ}\text{C}$

33 mV setting corresponds to  $793^{\circ}\text{C}$

34 mV setting corresponds to  $818^{\circ}\text{C}$

So that 32-34 represents a nominal furnace differential of  $50^{\circ}\text{C}$   
while 33-33 represents zero furnace temperature differential.

TABLE 3. SERIES 'B' MEASUREMENTS WITH DIFFERENTIAL THERMOCOUPLE PROBE (NOMINAL TEMPERATURE 800°C)

	Furnace settings (mV)	Absolute readings probe ( $\mu\text{V}$ )		Relative readings probe ( $\mu\text{V}$ )		Baseline drift ( $\mu\text{V}/\text{hour}$ )
		$(T_p)_1$	$(T_p)_2$	$\Delta T_p$	$\left(\frac{\Delta T_s}{\Delta x}\right) ^\circ\text{C}/\text{cm}$	
9/7/75	33-33	361.5	345	16.5	1.99	+1.8
	32-34			16.5	1.99	
	33-33		345			
	33-33	367.1	350	17.1	2.04	
	32-34			15.3	1.84	
	33-33		351.8			

TABLE 4. SERIES 'C' MEASUREMENTS WITH DIFFERENTIAL THERMOCOUPLE PROBE (NOMINAL TEMPERATURE 800°C)

	Furnace settings (mV)	Absolute readings probe ( $\mu\text{V}$ )		Relative readings probe ( $\mu\text{V}$ )		Baseline drift ( $\mu\text{V}/\text{hour}$ )
		$(T_p)_1$	$(T_p)_2$	$\Delta T_p$	$\left(\frac{\Delta T_s}{\Delta x}\right) ^\circ\text{C}/\text{cm}$	
15/7/75	33-33	198.6	179.7	18.9	2.27	+8
	32-34					
	32-34	219.0		19.5	2.34	
	33-33		199.5			
	33-33		209.7	21.3	2.56	
	32-34	231.0				
18/7/75	Large drift, but average of 4 changes gives				4.04	+11
19/7/75	33-33	235.6	199.0	36.6	4.65	Zero
	32-34					
	33-33		195.0	45.3	5.43	
	32-34	240.3		41.4	4.95	
	33-33	227.4	186.0			

These 3 runs on 19/7/75 were done with the probe in different positions in the melt.

TABLE 5. SERIES 'C' MEASUREMENTS WITH DIFFERENTIAL  
THERMOCOUPLE PROBE (NOMINAL TEMPERATURE 700°C)

	Furnace settings (mV)	Absolute readings probe ( $\mu$ V )		Relative readings probe ( $\mu$ V )		Baseline drift ( $\mu$ V/hour )
		$(T_p)_1$	$(T_p)_2$	$\Delta T_p$	$\left(\frac{\Delta T_s}{\Delta x}\right) ^\circ\text{C/cm}$	
18/7/75	29-29 28-30	194.0	159.0	35.0	4.20	Zero

TABLE 6. MEASUREMENTS IN HYDROGEN WITH DIFFERENTIAL  
THERMOCOUPLE PROBE (NOMINAL TEMPERATURE 800°C)

	Furnace settings (mV)	Absolute readings probe ( $\mu$ V )		Relative readings probe ( $\mu$ V )		Baseline drift ( $\mu$ V/hour )
		$(T_p)_1$	$(T_p)_2$	$\Delta T_p$	$\left(\frac{\Delta T_s}{\Delta x}\right) ^\circ\text{C/cm}$	
19/7/75	33-33 32-34	229.2	162.6	66.6	8.0	Zero

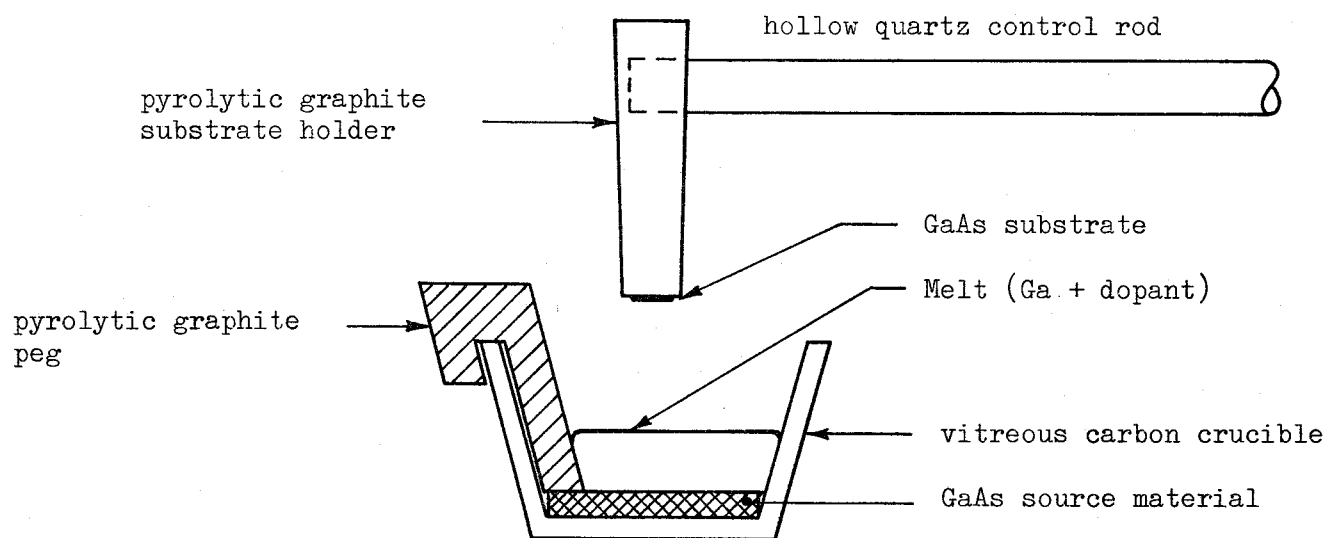
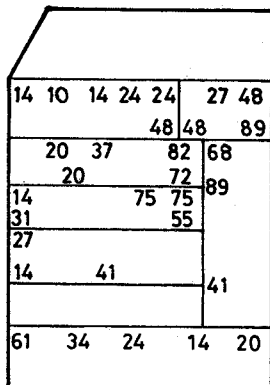
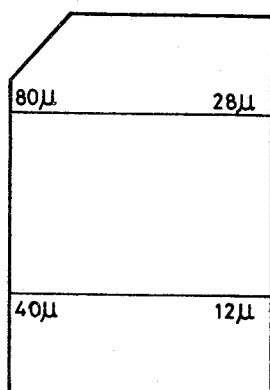


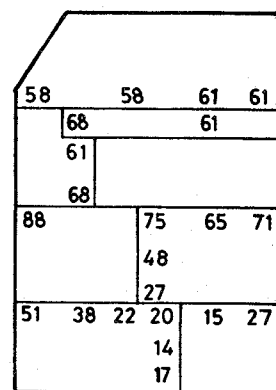
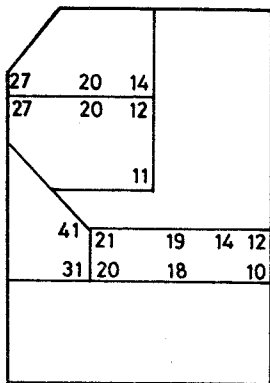
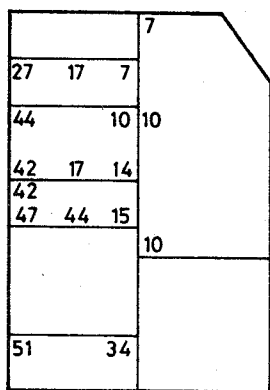
Figure 1. Schematic diagram of the growth vessel used for epitaxial layer growth by the Steady State method

800°C for 2 hours

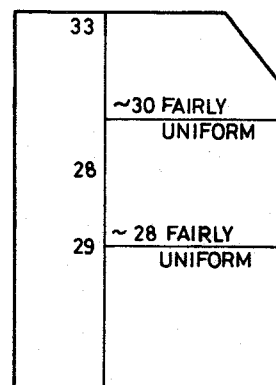
Bottom =  $817^{\circ}$

$$\approx 15 \mu/\text{hour}$$
Run 5  $\Delta x = 4 \text{ mm}$ Run 8  $\Delta x = 2.6$  mm

Run 9  $\Delta x = 2.5$  mm

Run 10  $\Delta x = 5 \text{ mm}$ Run 13  $\Delta x = 2.8$ 

Run 15  $\Delta x = 5 \text{ mm}$



700°C for 4 hours

Bottom = 721°

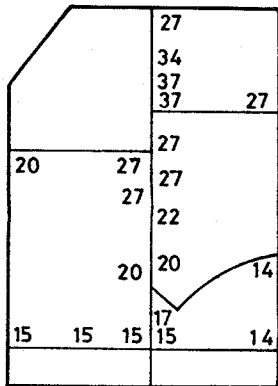
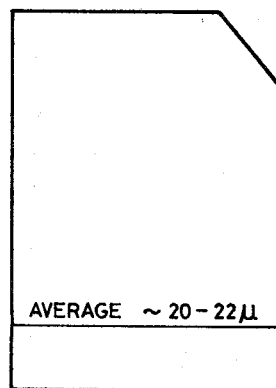
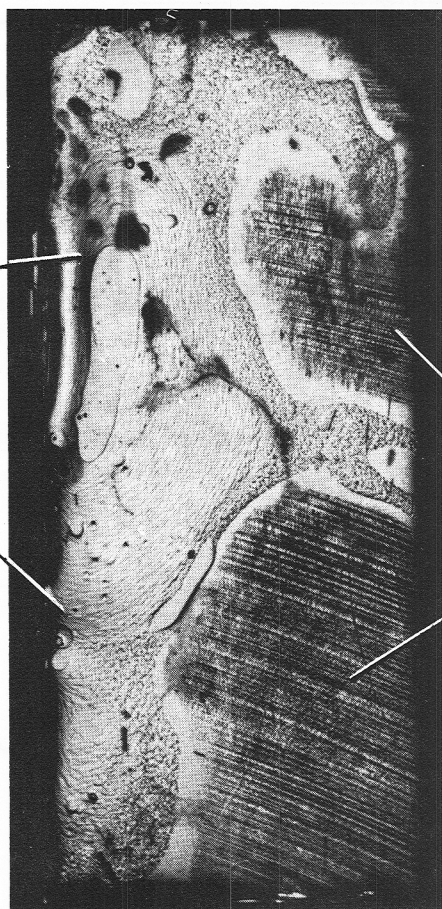
 $\approx 5 \mu / \text{hour}$ Run 11  $\Delta x = 5$  mmRun 14  $\Delta x = 5 \text{ mm}$ 

Figure 2. Schematic representation of spot heights for epitaxial layers grown at "average" temperatures of 800°C and 700°C. The left hand side of each diagram represents the edge of the substrate which was closest to the graphite peg used to hold the source block in position in the bottom of the growth vessel.

Non-uniform  
growth (close  
to graphite  
peg)



Etching in hotter  
region (distant  
from graphite  
peg)

Figure 3. Example of non-uniform epitaxial growth and simultaneous etching of the substrate surface, caused by large horizontal temperature gradients in the melt solution (Sample 17, nominally 700°C for 4 hours)

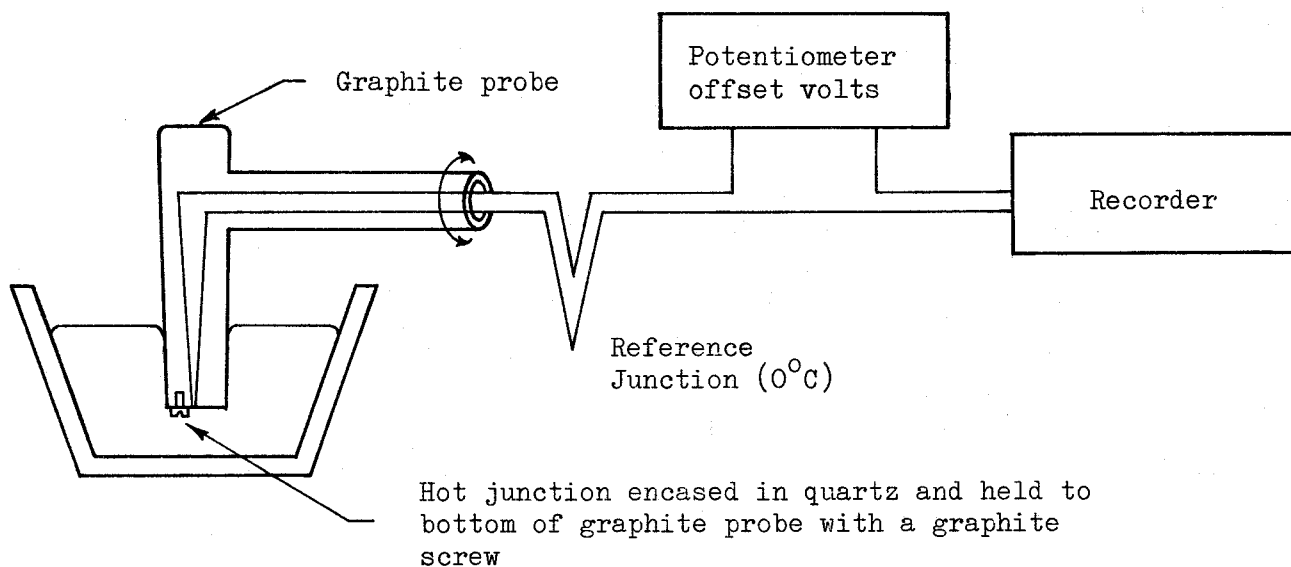


Figure 4. Schematic of the temperature measuring system used with the single thermocouple probe

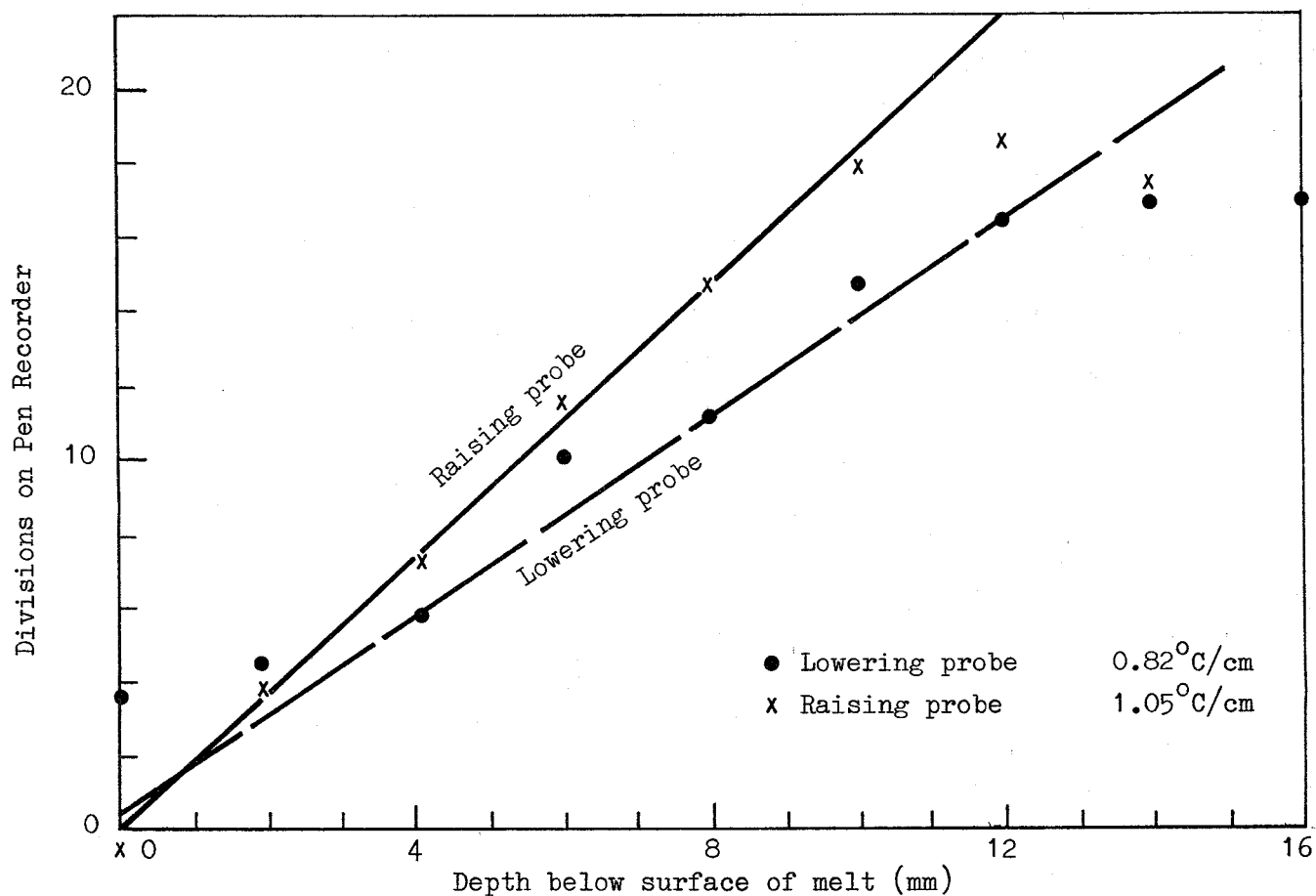


Figure 5. Typical example of the variation in results when the single thermocouple probe is lowered into or raised up out of the melt (40 divisions on the recorder =  $100\ \mu\text{V}$  from probe =  $2.4^{\circ}\text{C}$ )

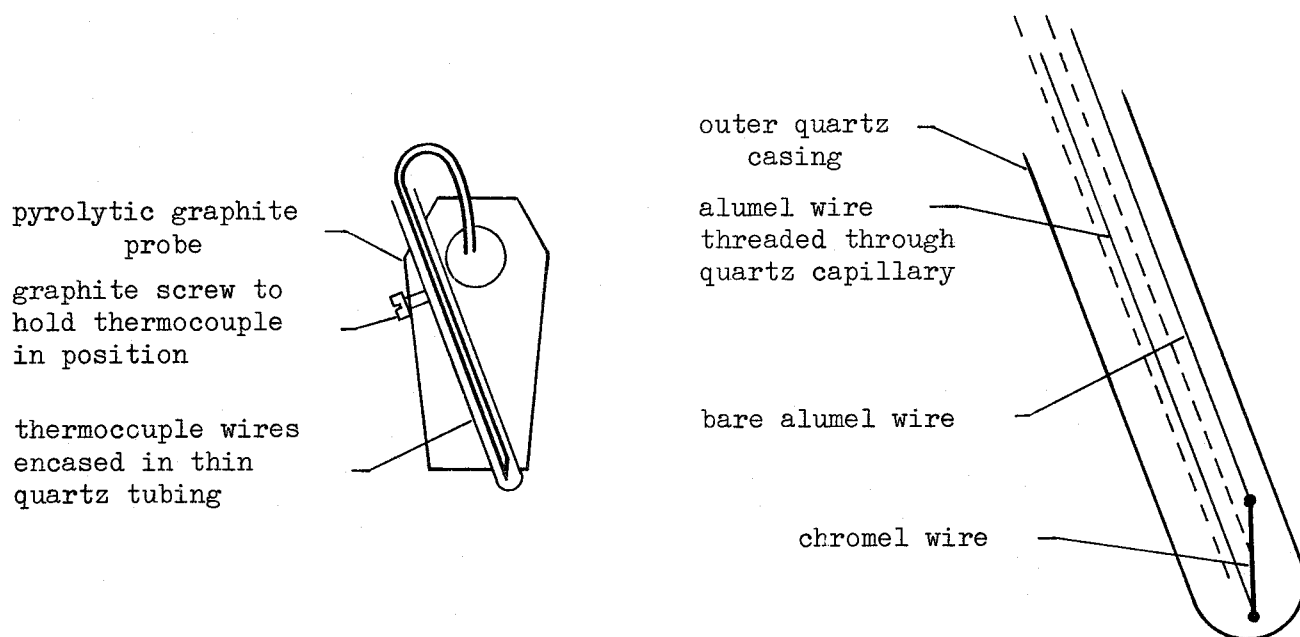


Figure 6(a). Schematic of the differential thermocouple probe assembly

Figure 6(b). Enlarged view of the differential probe. The vertical distance between the two chromel-alumel junctions is 2.0 mm

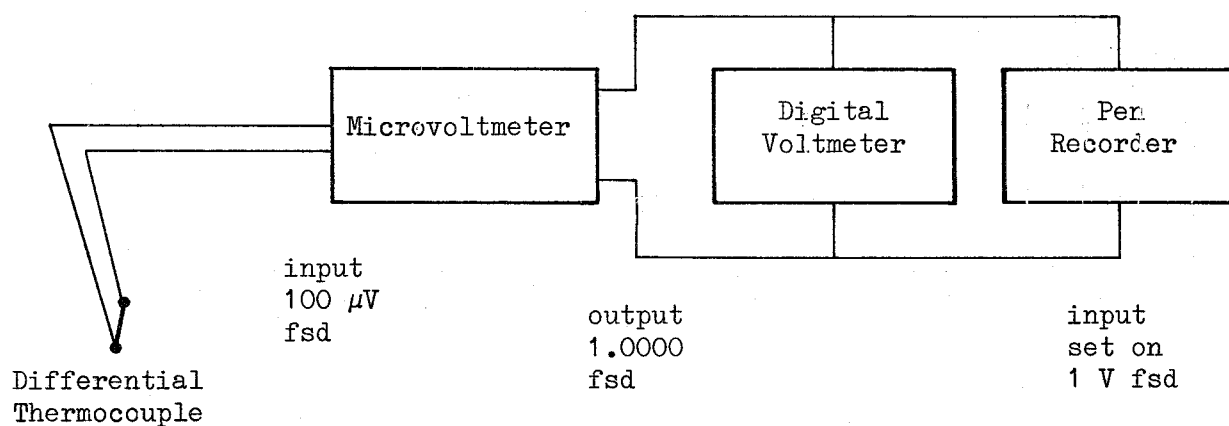


Figure 7. Technique used to increase the measurement accuracy of the differential thermocouple probe

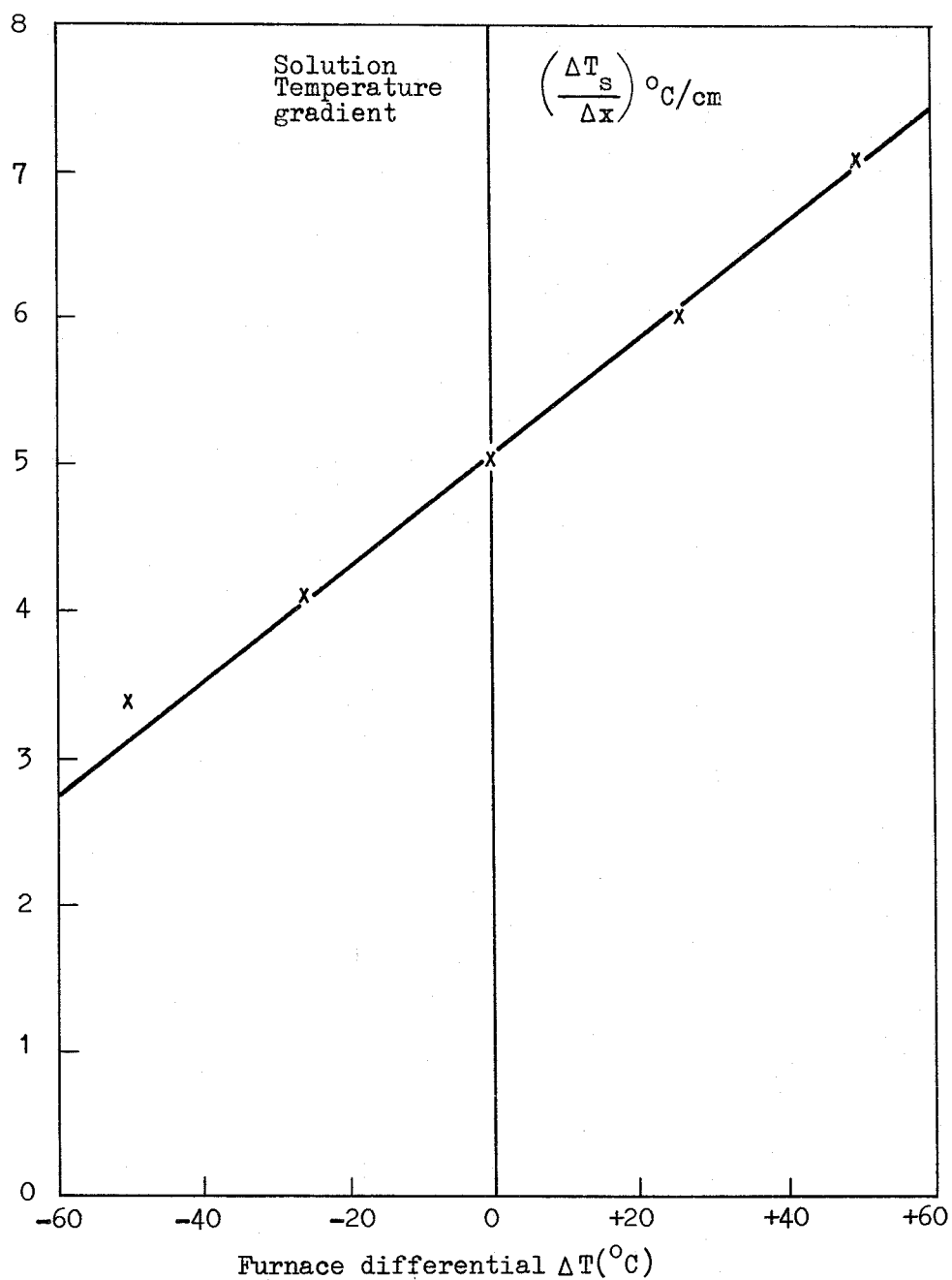


Figure 8. The linear relationship between the temperature gradient in the melt  $\left(\frac{\Delta T_s}{\Delta x}\right)$  and the applied furnace differential  $\Delta T$ . For a range of temperature differentials of  $-50^{\circ}\text{C}$  to  $+50^{\circ}\text{C}$ , the average slope  $\left(\frac{\Delta T_s}{\Delta x}\right) / \Delta T$  is  $3.85 \times 10^{-2}/\text{cm}$ .

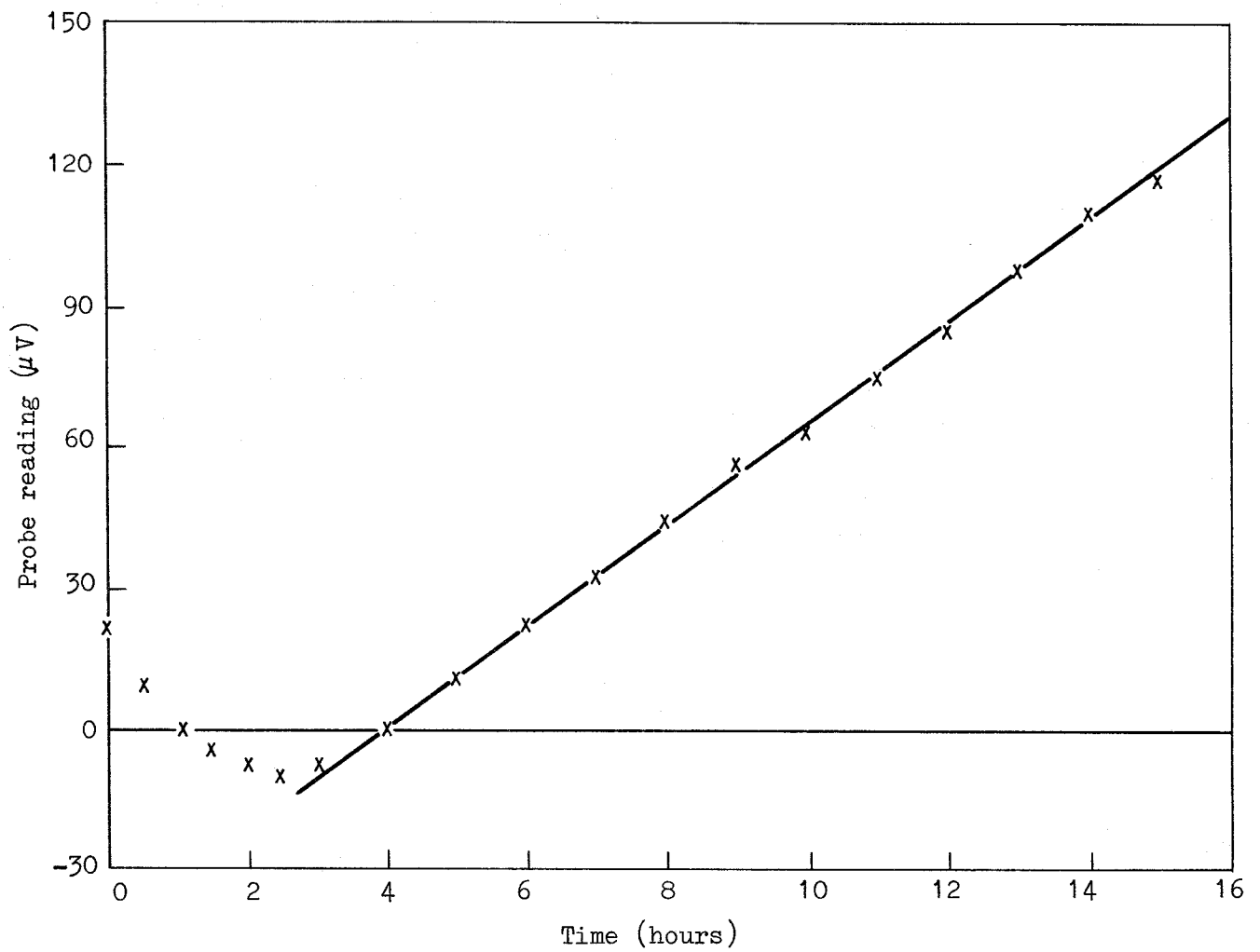


Figure 9. Magnitude of the baseline "zero" drift on one occasion, when both top and bottom furnace temperature controllers were set on 33 mV (793°C) (average drift over the linear region shown is 10.6 μV/hour)

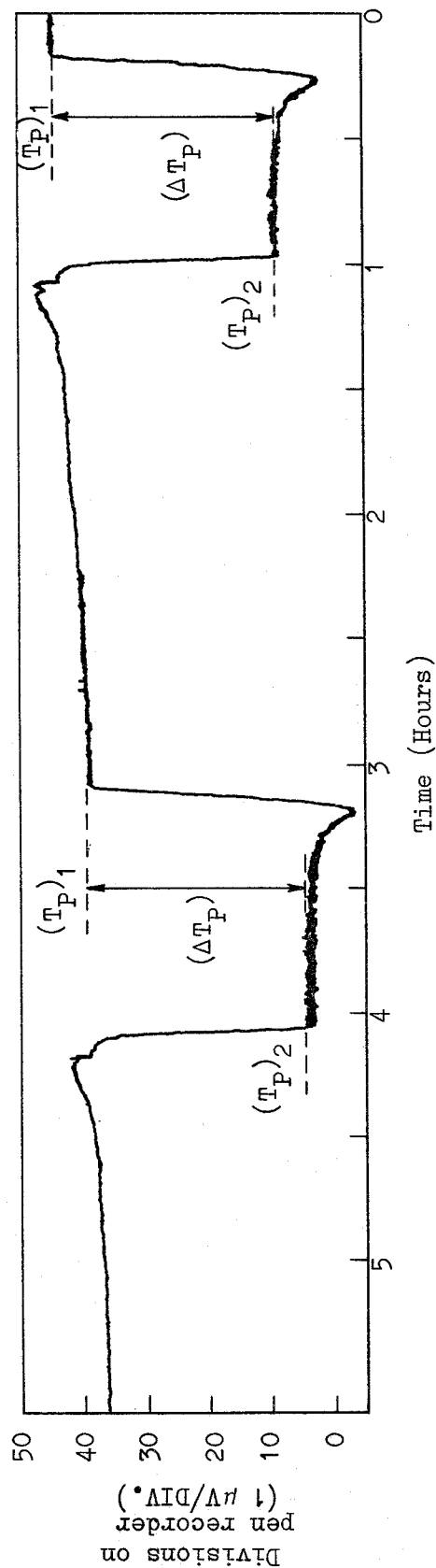


Figure 10. Recorder trace from the differential thermocouple probe at an "average" temperature of  $800^{\circ}\text{C}$ . The furnace settings used to determine the baseline were  $T_{\text{top}} = T_{\text{bottom}} = 33 \text{ mV}$  ( $793^{\circ}\text{C}$ ) while those used for a nominal differential  $\Delta T$  of  $50^{\circ}\text{C}$  were  $T_{\text{top}} = 32 \text{ mV}$  ( $769^{\circ}\text{C}$ ) and  $T_{\text{bottom}} = 34 \text{ mV}$  ( $818^{\circ}\text{C}$ ). The trace also demonstrates a typical baseline "zero" drift, in this example the drift is of magnitude  $\sim 2.3 \mu\text{V}/\text{hour}$

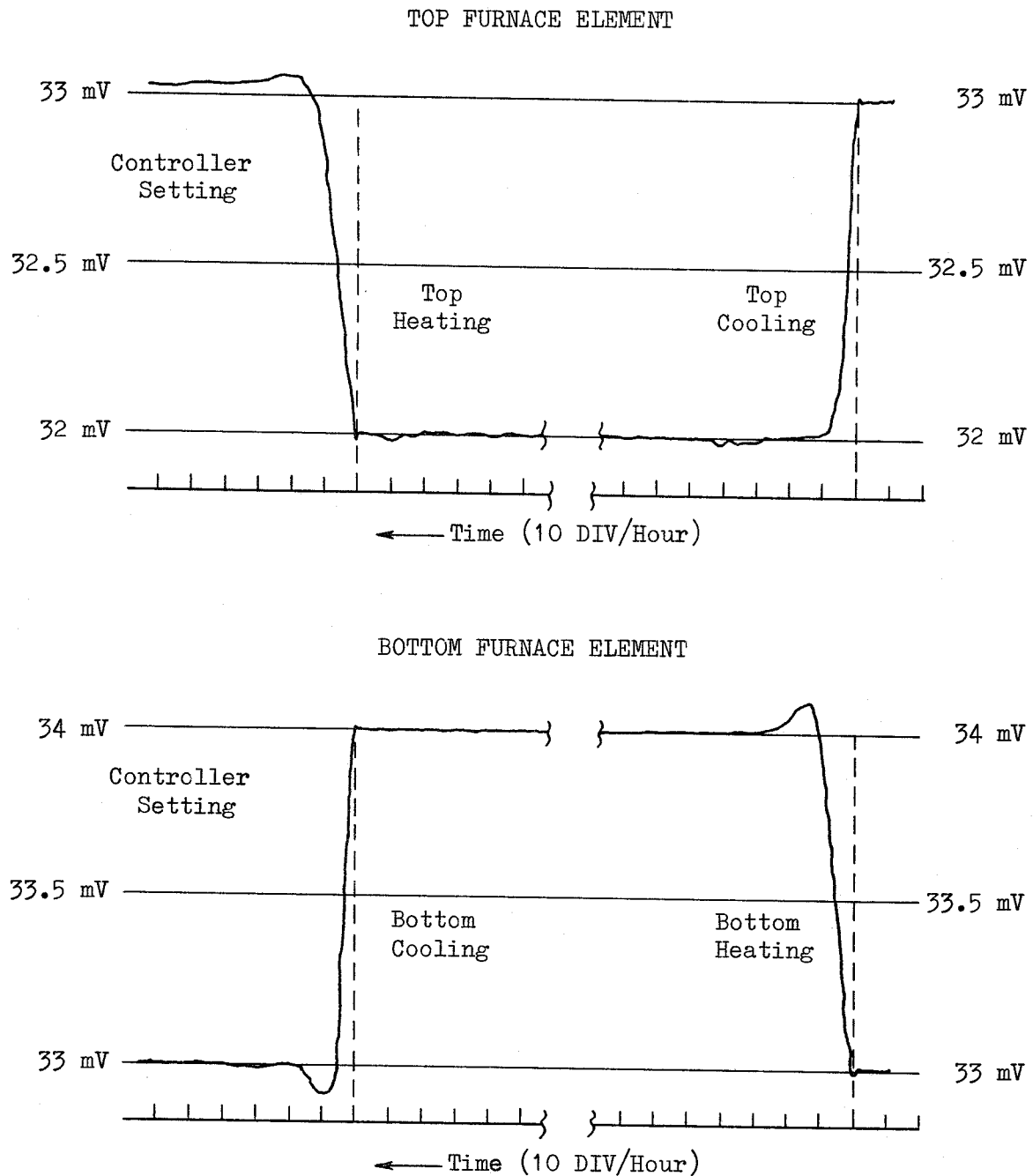


Figure 11. Temperature "overshoots" produced in the furnace by alteration of the top or bottom furnace temperature controllers

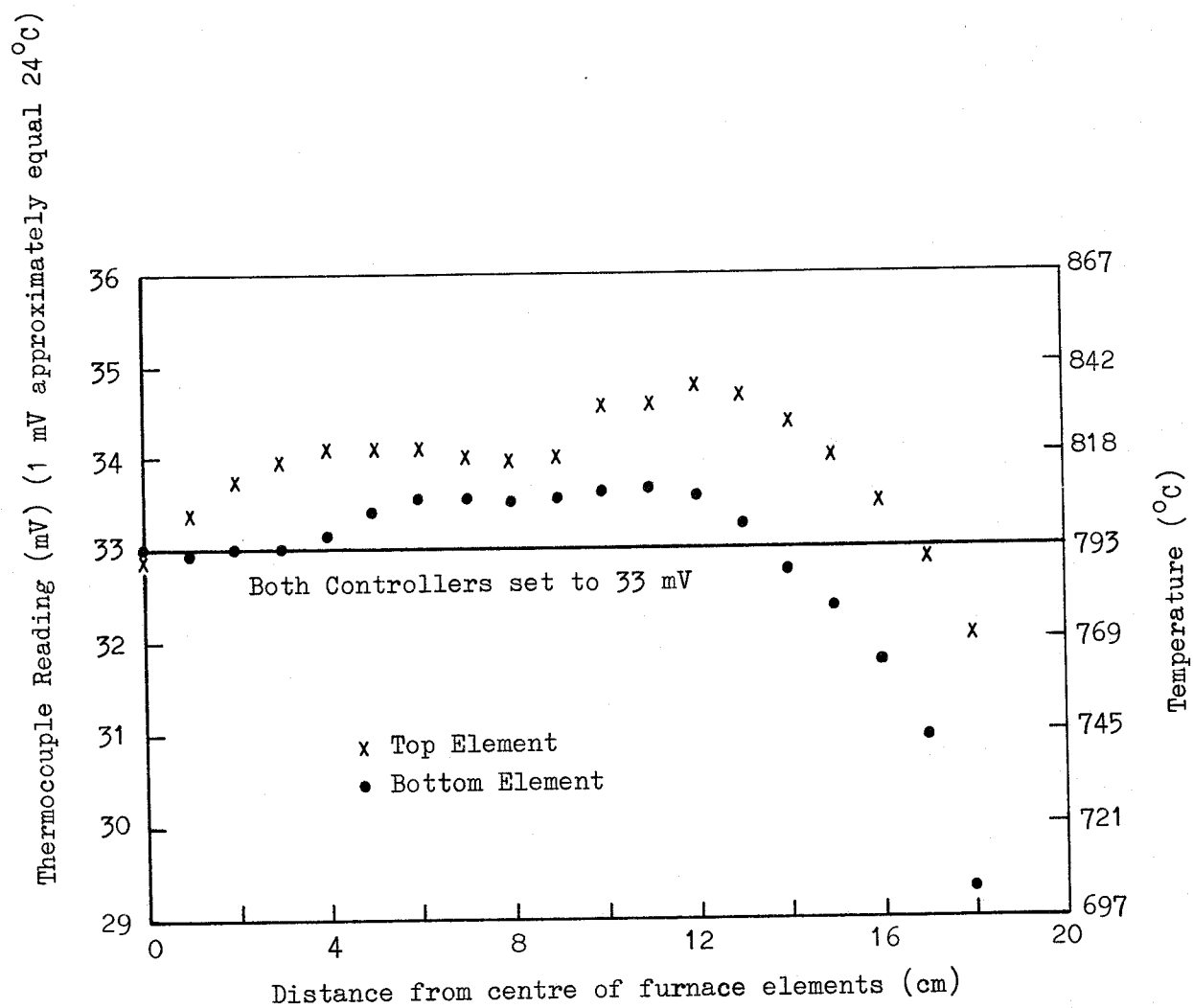


Figure 12. Axial variation of temperature along the furnace sections when both controllers are set to 33 mV (corresponding to 793°C)

## DOCUMENT CONTROL DATA SHEET

Security classification of this page

UNCLASSIFIED

1	DOCUMENT NUMBERS	2	SECURITY CLASSIFICATION
AR Number: AR-001-667		a. Complete Document: Unclassified	
Report Number: ERL-0077-TR		b. Title in Isolation: Unclassified	
Other Numbers:		c. Summary in Isolation: Unclassified	
3	TITLE		
THE MEASUREMENT OF TEMPERATURE INSTABILITIES AND THEIR EFFECT ON THE LIQUID PHASE EPITAXIAL GROWTH OF GALLIUM ARSENIDE			
4	PERSONAL AUTHOR(S):	5	DOCUMENT DATE:
M. Folkard		August 1979	
		6	6.1 TOTAL NUMBER OF PAGES 24
		6.2 NUMBER OF REFERENCES: 8	
7	7.1 CORPORATE AUTHOR(S):	8	REFERENCE NUMBERS
Electronics Research Laboratory		a. Task:	
7.2 DOCUMENT SERIES AND NUMBER		b. Sponsoring Agency:	
Electronics Research Laboratory 0077-TR		9	COST CODE:
		313338	
10	IMPRINT (Publishing organisation)	11	COMPUTER PROGRAM(S) (Title(s) and language(s))
Defence Research Centre Salisbury			
12	RELEASE LIMITATIONS (of the document):		
Approved for Public Release			
12.0	OVERSEAS	NO	P.R. 1 A B C D E

Security classification of this page:

UNCLASSIFIED

## 13 ANNOUNCEMENT LIMITATIONS (of the information on these pages):

No limitation

## 14 DESCRIPTORS:

a. EJC Thesaurus	Gallium arsenide	Process
Terms	Epitaxy	control
Temperature	Crystal growth	
control	Substrates	
	Semiconductors (Materials)	
	Thin films	
b. Non-Thesaurus	Liquid phase epitaxy	
Terms		

## 15 COSATI CODES:

2012

## 16 LIBRARY LOCATION CODES (for libraries listed in the distribution):

## 17 SUMMARY OR ABSTRACT:

(if this is security classified, the announcement of this report will be similarly classified)

Epitaxial layers grown on gallium arsenide substrates using the steady state temperature gradient form of liquid phase epitaxy have a much larger growth rate than that calculated for diffusion-limited conditions. In addition, and of major importance for device fabrication, there is a large variation in epilayer thickness over the surface of a single sample, and non-reproducibility from sample to sample.

The present report describes various measurements of the temperature and its local variation within the gallium melt solution, and attempts to relate the observed variations and instabilities to the epitaxial layers actually grown.